A modified Xinanjiang model and its application in northern China

Caihong Hu, Shenglian Guo, Lihua Xiong and Dingzhi Peng

State Key Laboratory of Water Resources and Hydropower Engineering Science, Wuhan University, Wuhan 430072, People's Republic of China. E-mail: *guosl@hbstd.gov.cn*; *Slguo@peoplemail.com.cn*

Received 1 July 2003; accepted in revised form 15 June 2004

Abstract The Xinanjiang model has been widely used in the humid regions in southern China as a basic tool for rainfall–runoff simulation, flood forecasting and water resources planning and management. However, its performance in the arid and semi-arid regions of northern China is usually not so good as in the humid regions. A modified Xinanjiang model, in which runoff generation in the watershed is based on both infiltration excess and saturation excess runoff mechanisms, is presented and discussed. Three different watersheds are selected for assessing and comparing the performance of the Xinanjiang model, the modified Xinanjiang model, the VIC model and the TOPMODEL in rainfall–runoff simulation. It is found that the modified Xinanjiang model performs better than the Xinanjiang model, and the models considering the Horton and Dunne runoff generation mechanisms are slightly better than those models considering the single runoff generation mechanism in semi-arid areas. It is suggested that the infiltration excess runoff mechanism should be included in rainfall–runoff models in arid and semi-arid regions.

Keywords Modified Xinanjiang model; rainfall–runoff modeling; TOPMODEL; VIC model; Xinanjiang model

Nordic Hydrology **Vol 36 No 2 pp 175–192** © IWA Publishing 2005

Introduction

Since Crawford and Linsly (1966) put forward the Stanford Watershed Model, there has been a proliferation of watershed models (Singh 1995; Singh and Frevert 2002), such as the API-type hydrological model (Sittner *et al.* 1969), the Danish NAM model (Nielsen and Hansen 1973), the Swedish HBV model (Bergström and Forsman 1973), the SACramento model (Burnash *et al.* 1973), the Tank model (Sugawara 1974) the TOPMODEL (Beven and Kirkby 1979), the HEC-1 (Feldman 1981), the SSARR model of the US Corps of Engineers (Rockwood 1982), the Xinanjiang model (Zhao 1980, 1992), the ARNO model (Todini 1996) and the VIC model (Liang and Lettenmaier 1994; Liang *et al.* 1996; Liang and Xie 2001, 2003), etc. These models are of different types and were developed for different purposes. Traditionally, hydrological models can be classified as physically based or conceptual, depending on the degree of complexity and physical completeness in the formulation of the structure (Beven 1989; Bergström 1991; Singh 1995; Refsgaard 1996). Models are also classified as lumped or distributed, depending on the degree of discretization in describing the terrain in the basin. The conceptual approach to simulate discharges at the outlet of a watershed is based on modeling the watershed behavior through recognition of the physical processes involved in the transformation of rainfall into river flow. In general, conceptual models only indirectly take into account the spatial variability of processes, input, boundary conditions and system (watershed) geometric characteristics. Conceptual rainfall–runoff models are normally run with precipitation and potential evapotranspiration as the primary input data, and they produce watershed values of evaporation, soil moisture and runoff, which is very important in regions where precipitation data series are available but runoff data are scarce. Conceptual models, depending on the calibration for their

parameter values, with little or no physical meaning, can simulate entire hydrological processes occurring in watersheds, and are used extensively in watershed hydrology.

The World Meteorological Organization sponsored three studies on the intercomparison of watershed hydrological models (WMO 1975, 1986, 1992). Apart from the WMO reports, some efforts have been made to compare models of some component processes (Franchini and Pacciani 1991). Also, model developers usually compare their models with one or two other models. One of the main conclusions has been that all kinds of models, whether simple or complex, can have good results in the humid regions, but for arid and semi-arid regions the model must be carefully selected. In semi-arid regions, the more complex, explicit soil-moisture-accounting models perform in a manner which is demonstrably superior to the simpler, implicit soil-moisture-accounting types (WMO 1975, 1986).

The First National Hydrological Forecasting Technology Competition of China was held in 1997, and ten models and six watersheds were selected for this competitive study. Those models were the Xinanjiang model, the Jiangwang Runoff model, the Double Excesses Runoff Generation model, the Hebei Rainfall-runoff model, the Double Attenuation Curve model, the Synthesized Constrained Linear System (SCLS), the API, the NAM, the SAC and the TANK model. The conclusions were that almost all models, simple or complex, have good flexibility in humid regions, and some models considering the infiltration excess have more adaptability in humid regions. But the rainfall–runoff process was simulated poorly in semi-arid and semi-humid regions, especially in semi-arid regions (Li 1998).

In general, regardless of the complexity or simplicity of the models, they can make more accurate predictions in humid regions, where subsurface runoff and saturation excess runoff components dominate. In semi-humid and semi-arid regions, rainfall will frequently be less than potential evaporation, and infiltration excess runoff and saturation excess runoff always interact together to varying degrees. Atkinson *et al.* (2002) studied the minimum level of model complexity necessary to guarantee the accuracy of rainfall–runoff modeling in four New Zealand watersheds. They found that dry watersheds are sensitive to a threshold storage parameter, producing inaccurate results with little confidence, while humid watersheds are relatively insensitive, producing more accurate results with more confidence. Sensitivity to the threshold parameter is well correlated with climate and timescale. As mentioned by Farmer *et al.* (2003), drier catchments are shown to be more sensitive to small-scale perturbations than humid catchments. Therefore, the mechanism of rainfall–runoff generation is more complex in semi-arid and semi-humid regions than that in humid ones, and these regions are also scarce in hydrological data.

This paper presents a modified Xinanjiang model that considers both saturation excess runoff and infiltration excess runoff generation mechanisms for rainfall–runoff simulation in semi-arid and semi-humid regions. A comparison study is also conducted involving application of the original Xinanjiang model, the VIC model and the TOPMODEL to three watersheds in semi-arid and semi-humid regions in northern China.

The modified Xinanjiang model

The Xinanjiang model (Zhao 1980, 1992), which uses precipitation and potential evaporation data to compute actual evapotranspiration, soil moisture storage, surface runoff, interflow and groundwater runoff from the watershed, is by far the most important conceptual rainfall–runoff model in China and has been successfully used for flood forecasting. The evapotranspiration component is calculated by a three soil layer model. Runoff production occurs in repletion of storage to capacity values which are assumed to be distributed throughout the basin. The interflow and the groundwater flow are routed through linear reservoir methods. Runoff concentration to the outflow is represented by a unit hydrograph or by a lag routing technique. Since its appearance, the Xinanjiang model

has been modified in order to adapt it to a wide range of applications, such as runoff separation into three or four components (Wang 1982; Hu *et al.* 1986; Wang and Zhao 1989). Todini (1988, 1996) found that a major improvement could be obtained by allowing the soil moisture to be depleted not only by evaporation, as in the original Xinanjiang model, but also by percolation into the water table, as proposed in the ARNO model. Luo *et al.* (1992) proposed a modified Xinanjiang model that considers both Dunne (saturation excess) runoff and Horton (infiltration excess) runoff generation mechanisms. Liang and Lettenmaier (1994), Liang *et al.* (1996) and Liang and Xie (2001) presented and developed the VIC (variability infiltration capacity) model that takes into account the effects of spatial variability of the soil infiltration rate and soil moisture capacity on Horton and Dunne runoff at different locations of a studied area. The total surface runoff is the sum of Dunne runoff and Horton runoff. The modified Xinanjiang model is described and discussed as follows.

General description

A considerable amount of research on mechanisms of runoff generation has been carried out (Kirkby 1978; Dunne 1978; Zhao 1980; Luo *et al.* 1992; Liang *et al.* 1996; Rui and Jiang 1997). Numerous studies have shown that quick flow runoff in actual watersheds is generated by these mechanisms: infiltration excess runoff (Horton flow), saturation excess runoff (Dunne flow) and rapid groundwater flow. Infiltration excess runoff is generated from locations where the rainfall duration is longer than the required ponding time such that the rainfall rate exceeds the saturated hydraulic conductivity of the surface soil. Saturation excess runoff takes place when the saturated hydraulic conductivity of the surface soil is high and the initial groundwater table is shallow (Dunne 1978). Surface saturation occurs because of the rising groundwater table, and overland flow occurs when no further soil moisture storage is available (Freeze 1980). Abdul and Gillham (1984) found that the importance of the capillary fringe on the saturation excess mechanism of runoff production and the correlation between runoff contributing areas and the seepage face and the expansion of the seepage face and the rise in the water table also contributed to an increase of the rapid groundwater response during rainfall events. Beldring (2002) demonstrated that groundwater flow in many cases is the dominating component of quick flow. Dunne (1978) also demonstrated that, even within a particular watershed, the dominant runoff producing mechanism might vary with storm characteristics and antecedent conditions. Different mechanisms may be operative both at the same or different times and at the same or different locations. The spatial variability of soil properties and topography may also result in different runoff generation mechanisms. Zhao (1980) pointed out that the Horton runoff generation would occur under dry soil conditions and high intensity rainfall, and saturation excess runoff primarily in humid regions. The infiltration excess runoff and the groundwater flow are the main components in tilled soil regions (Beldring *et al.* 1999; Beldring 2002), while the runoff generation in semi-arid and semi-humid regions is different from that in arid and humid regions. There is a large heterogeneity in soil types over a watershed and the very complex hydrological response at the land surface. The infiltration excess runoff tends to dominate overland flow production, depending on rainfall intensity, where the absence of vegetation and other factors prevent water from moving easily; the saturation excess runoff tends to occur after a shallow saturated layer has been built up due to a lack of soil depth, or to the presence of a less permeable layer (Sivapalan *et al.* 1987).

The runoff generation mechanism is complex in semi-humid and semi-arid regions, especially in semi-arid regions, where two runoff generation mechanisms, saturation excess runoff and infiltration excess runoff, are interacting together. Both the infiltration excess runoff and the saturation excess runoff can be concurrent in rainfall–runoff events.

Infiltration and saturation excess runoff can be present at different locations or different times due to the spatial variability of soil infiltration rate and soil moisture capacity. The original Xinanjiang model takes account of saturation excess runoff generation through a probability distribution function of soil storage capacity. Therefore, this suggests that it should be possible to expand the model approach considerably to also allow for infiltration excess runoff generation. However, the key to establishing a rainfall–runoff model in semi-arid and semi-humid regions is to solve the problem of the uneven distribution of runoff generation when the rainfall is assumed to be even. The distribution of runoff generation is uneven because of the non-uniform distribution of soil moisture deficit or infiltration intensity over the watershed. The modified Xinanjiang model takes account of the effects of the spatial distribution of infiltration and adopts the soil infiltration capacity curve to accommodate the non-uniformity of the soil infiltration based on the original Xinanjiang model (Luo *et al.* 1992). The modified Xinanjiang model structure will be described in this section. Figure 1 shows the flow chart of the modified Xinanjiang model.

The modified Xinanjiang model considers both Horton and Dunne runoff generation mechanisms simultaneously and assumes that the Horton runoff occurs if the rainfall intensity rate is greater than the infiltration rate, while the Dunne runoff occurs if the soil moisture reaches the field capacity. The saturation excess runoff in this model is computed following the concepts of the original Xinanjiang model (Zhao 1980, 1992). The spatial variation of soil moisture capacity is expressed by a spatial probability distribution as follows:

$$\alpha = 1 - \left(1 - \frac{W'}{W'_m}\right)^b \tag{1}$$

where W' and W'_m are the point soil moisture capacity and maximum point soil moisture capacity, respectively, α is the area fraction in which the soil moisture capacity is less than or equal to W' and b is an empirical index.

Similar to the concept of spatial variation of soil moisture capacity over the watershed, an infiltration capacity distribution curve, $F'_{\Delta t} \sim \beta$, is adopted for estimating the infiltration

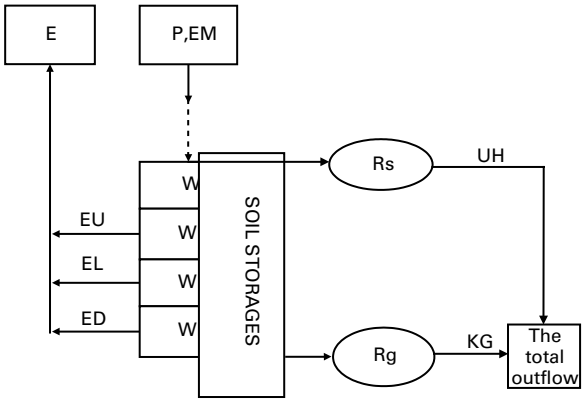

Figure 1 Flow chart for the modified Xinanjiang model. (P - precipitation, EM - potential evaporation, Rs – surface runoff, Rg – groundwater runoff, W – total soil moisture, WU – upper layer soil moisture, WL – lower layer soil moisture, WD – deeper layer soil moisture, EU – upper layer soil evaporation, EL – lower layer soil evaporation, ED – deeper layer soil evaporation, E – actual evaporation, UH - unit hydrograph, KG – coefficient of groundwater runoff)

excess runoff. For a time interval Δt, the distribution curve of the infiltration capacity can be expressed as

$$\beta = 1 - \left(1 - \frac{F'_{\Delta t}}{F'_{m\Delta t}}\right)^m \tag{2}$$

where $F'_{\Delta t}$, $F'_{m\Delta t}$ are the point soil infiltration capacity and maximum soil infiltration capacity, respectively, m is an empirical index and β is the area fraction in which the soil infiltration capacity is less than or equal to $F'_{\Delta t}$. $F'_{\Delta t}$ varies from zero to a maximum $F'_{m\Delta t}$ according to Eq. (2). Therefore, the time-interval infiltration capacity of the watershed $F_{m\Delta t}$ is defined as the average infiltration capacity of the time interval Δt for the watershed when the water supply is sufficient (see Figure 2).

Horton's infiltration equation is adopted as the spatially averaged point infiltration function in this model. Thus we have

$$f = f_c + (f_0 - f_c)e^{-kt} \tag{3}$$

where f_c is a final or equilibrium capacity (m/h), f_0 is the initial infiltration capacity (m/h) and k is a constant representing the rate of decrease in f capacity. It indicates that, if the rainfall supply exceeds the infiltration capacity, infiltration tends to decrease in an exponential manner.

So the average time interval infiltration capacity of a watershed, $F_{m\Delta t}$, can be derived by integrating Eq. (3) over the time interval Δt as follows:

$$F_{m\Delta t} = \int_t^{t+\Delta t} f dt = f_c \Delta t + \frac{1}{k}(f_0 - f_c)e^{-kt}(1 - e^{-k\Delta t}) \tag{4}$$

$F_{m\Delta t}$, the average infiltration capacity, can also be derived by integreting over the area under the time-interval infiltration capacity curve, which can be expressed as

$$F'_{m\Delta t} = (m+1)F_{m\Delta t} \tag{5}$$

The infiltration excess runoff generated over the watershed is due to the variability of soil heterogeneity. This is not considered in the original Xinanjiang model. The basic structure of the modified Xinanjiang model is shown in Figure 3. $F'_{\Delta t} \sim \beta$ is superimposed on the

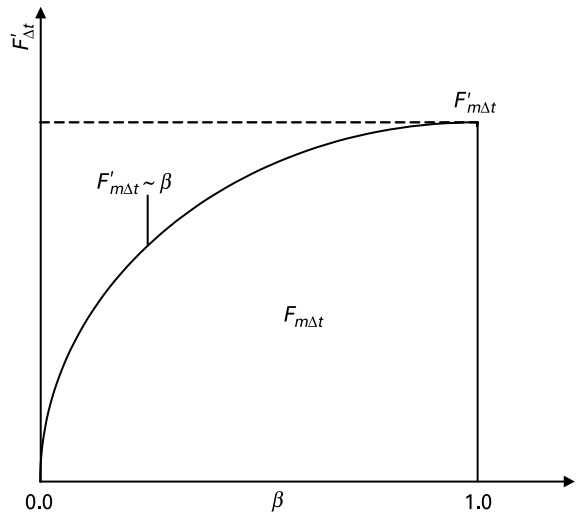

Figure 2 Distribution curve of infiltration capacity for any time interval

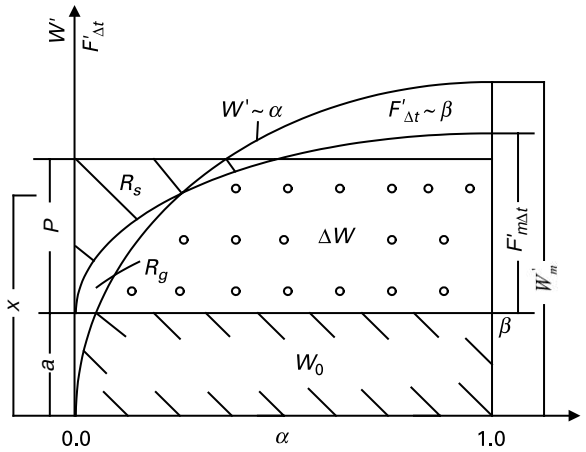

Figure 3 Schematic diagram of runoff generation of the modified Xinanjiang model

horizontal a, where it is assumed that the distribution of actual storage in the watershed W_0 will be characterized (see Figure 3). The distribution curve of the infiltration capacity, $F'_{\Delta t} \sim \beta$, divides the watershed into two parts: β and $1 - \beta$. The surface runoff R_s (represented by the diagonal shaded areas in Figure 3) is generally produced by the area fraction β, in which the infiltration capacity is exceeded by the precipitation rate; the other fraction, $1 - \beta$ (represented by the blank and circle shaded areas in Figure 3) is the area fraction of un-infiltration excess, in which any runoff is not produced. While $W' \sim \alpha$, the moisture storage capacity curve, partitions the watershed into two parts: α and $1 - \alpha$, the groundwater runoff R_g (represented by the blank areas in Figure 3) is generated in the saturated area fraction α, in which the soil storage is saturated since the infiltrated water goes into soil storage. So the total runoff R is $R = R_s + R_g$ ΔW (represented by the circle shaded areas in Figure 3), the increased soil moisture, is depleted by the evaporation and does not produce runoff. $\Delta W = P - R$ according to the water balance equation.

Runoff generation

From the above description, it is clear that we need to find expressions of the total runoff (R), the surface runoff (R_s), the groundwater runoff (R_g) and soil moisture change (ΔW) at each time step according to Eqs. (1) and (2), given the amount of precipitation (P) for the same time period. According to the relations among variables, there are two conditions of runoff production (see Figures 4 and 5). Based on Eqs. (1) and (2), the surface runoff R_s, the groundwater runoff R_g and the total runoff R can be derived according to different conditions as follows, respectively.

(1) If $a + F'_{m\Delta t} \leq W'_m$, then there is an intersecting point of two distributed curves when the initial soil water is low (see Figure 4). x is the distance from the intersecting point to the abscissa α. In general, $b \geq m$, and at the intersecting point x, $\alpha = \beta$, so the value of x can be obtained as

$$x = a + F'_{m\Delta t}\left(1 - \left(1 - \frac{x}{W'_m}\right)^{b/m}\right) \tag{6}$$

where x can be calculated by the iterative method.

Then, the surface runoff (R_s) and the groundwater runoff (R_g) are obtained according to the following three kinds of conditions as shown in Figure 4(a), (b) and (c), and obtained by integrating the infiltration capacity distribution curve and the soil moisture capacity curve.

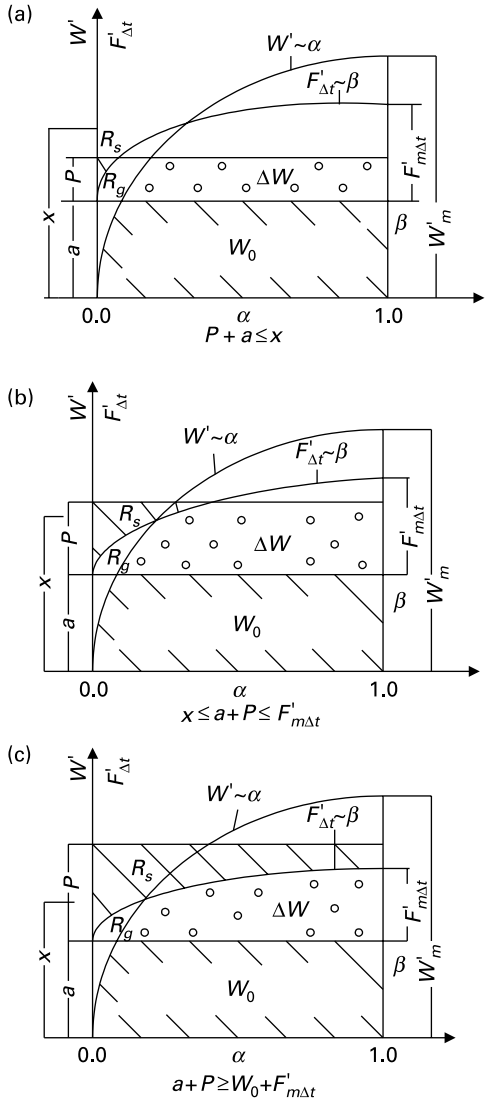

Figure 4 Schematic calculating runoff generation if $a + F'_{m\Delta t} \leq W'_m$

(a) If $a + P \leq x$, see Figure 4(a), based on Eqs. (1) and (2), R_s, R_g and R can be represented as follows, respectively:

$$R_s = \int_0^P \beta \mathrm{d}F'_{\Delta t} = P - F_{m\Delta t}\left[1 - \left(1 - \frac{P}{F'_{m\Delta t}}\right)^{m+1}\right] \tag{7}$$

$$R_g = \int_a^{a+P} \alpha \mathrm{d}W' - \int_0^P \beta dF'_{\Delta t}$$

$$= F_{m\Delta t}\left[1 - \left(1 - \frac{P}{F'_{m\Delta t}}\right)^{m+1}\right] - (W_m - W_0) + W_m\left(1 - \frac{a+P}{W'_m}\right)^{b+1} \tag{8}$$

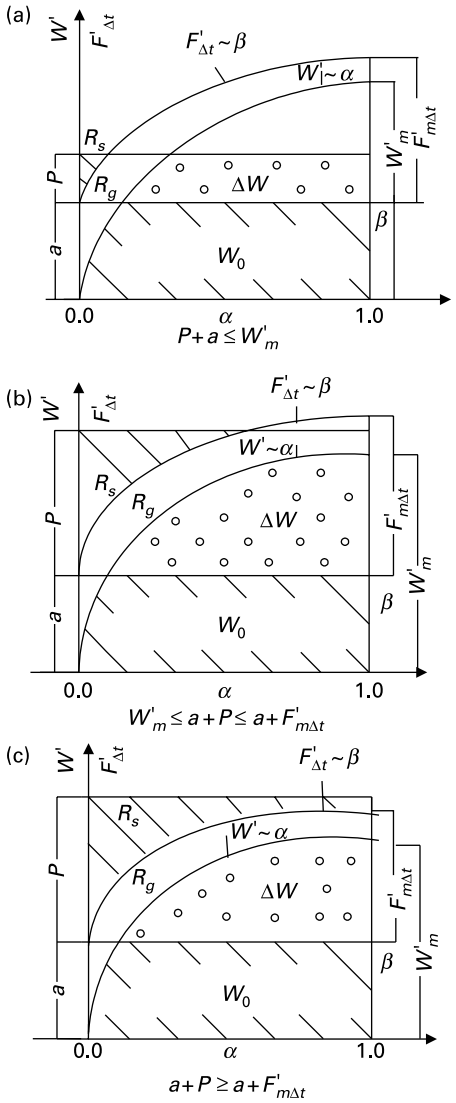

Figure 5 Schematic calculating runoff generation if $a + F'_{m\Delta t} > W'_m$

$$R = R_s + R_g = P - (W_m - W_0) + W_m\left(1 - \frac{a+P}{W'_m}\right)^{b+1} \tag{9}$$

(b) If $x \le a + p \le a + F'_{m\Delta t}$, see Figure 4(b).

The expression of R_s can be obtained by Eq. (7) because they have the same procedure of surface runoff generation:

$$R_g = \int_a^x \alpha \mathrm{d}W' - \int_0^{x-a} \beta \mathrm{d}F'_{\Delta t}$$

$$= F_{m\Delta t}\left[1 - \left(1 - \frac{x-a}{F'_{m\Delta t}}\right)^{m+1}\right] - (W_m - W_0) + W_m\left(1 - \frac{x}{W'_m}\right)^{b+1} \tag{10}$$

$$R = R_s + R_g$$

$$= P + F_{m\Delta t}\left(1 - \frac{P}{F'_{m\Delta t}}\right)^{m+1} - F_{m\Delta t}\left(1 - \frac{x-a}{F'_{m\Delta t}}\right)^{m+1} - (W_m - W_0)$$

$$+ W_m\left(1 - \frac{x}{W'_m}\right)^{b+1} \tag{11}$$

If $a + P \geq a + F'_{m\Delta t}$, see Figure 4(c):

$$R_s = P - \int_0^{F'_{m\Delta t}} (1-\beta)\mathrm{d}F'_{\Delta t} = P - F_{m\Delta t} \tag{12}$$

The expression of R_g can be obtained by Eq. (10):

$$R = R_s + R_g = P - (W_m - W_0) - F_{m\Delta t}\left(1 - \frac{x-a}{F'_{m\Delta t}}\right)^{m+1} + W_m\left(1 - \frac{x}{W'_m}\right)^{b+1} \tag{13}$$

(2) If $a + F'_{m\Delta t} > W'_m$, then there is no intersecting point of the two distributed curves when the initial soil water is high (see Figure 5). The runoff generation is calculated according to the following three kinds of conditions as shown in Figure 5(a), (b) and (c).

(a) If $a + P \leq W'_m$, see Figure 5(a). The runoff generation of R_s, R_g, and R have the same procedure with (1(a)), so R_s, R_g, and R can be obtained by Eqs. (7), (8) and (9), respectively.
(b) If $W'_m < a + P \leq a + F'_{m\Delta t}$, see Figure 5(b).

R_S can be obtained by Eq. (7):

$$R_g = \int_0^P (1-\beta)\mathrm{d}F'_{\Delta t} - (W_m - W_0)$$

$$= F_{m\Delta t}\left(1 - \left(1 - \frac{P}{F'_{m\Delta t}}\right)^{m+1}\right) - (W_m - W_0) \tag{14}$$

$$R = R_s + R_g = P - (W_m - W_0) \tag{15}$$

If $a + P \geq a + F'_{m\Delta t}$, see Figure 5(c):

$$R_s = P - \int_0^{F'_{m\Delta t}} (1-\beta)\mathrm{d}F'_{\Delta t} = P - F_{m\Delta t} \tag{16}$$

$$R_g = \int_0^{F'_{m\Delta t}} (1-\beta)\mathrm{d}F'_{\Delta t} = F_{m\Delta t} - (W_m - W_0) \tag{17}$$

R can be obtained by Eq. (15).

It can be seen from Eqs. (7)–(17) that the precipitation (or throughfall) P can be partitioned into R_s, R_g and ΔW through their relationships with the soil characteristics. As described above, two soil spatial distributions, Eqs. (1) and (2), are used simultaneously to represent the spatial heterogeneity of soil properties in the modified Xinanjiang model.

The modified Xinanjiang model has 12 parameters. They can be classified into evapotranspiration parameters K, WU_m, WL_m, C, runoff production parameters W_m, b, m, k, f_c and routing parameters cn, ck, K_g.

Model calibration and validation

For the modified Xinanjiang model, most of its parameters can only be quantified by calibration against historical records because of the uncertainty of the information on the soil characteristics. The combination of Genetic, Rosenbrock and Simplex optimization algorithms was used for the model's calibration in order to obtain the optimized parameters values. The Genetic algorithm is first used to calibrate the model: the calibrated results of the Genetic algorithm are then used as initial parameter values for the other two optimization methods for further calibration, and the parameters are finally optimized by the Simplex method.

The effectiveness of the calibration and validation was based essentially on a criterion of visual comparison between computed and observed discharges. The model performance was estimated through the Nash efficiency coefficient R^2 (Nash and Sutcliffe 1970) and the total runoff relatively error RE (Madsen 2002; Zhang and Guo 2002):

$$R^2 = \left(1 - \frac{\sum(Q_i - \hat{Q}_i)^2}{\sum(Q_i - \bar{Q}_c)^2}\right) \times 100 \tag{18}$$

$$RE = \left(\frac{\sum_i \hat{Q}_i}{\sum_i Q_i} - 1\right) \times 100 \tag{19}$$

where Q_i is the observed discharge (m^3/s), $\hat{Q}_i$ is the simulated discharge (m^3/s) and $\bar{Q}_c$ is the mean observed discharge in the calibration periods (m^3/s). Though these two criteria have some limitations, they are still the most widely used indices in rainfall–runoff simulation for calibrating model parameters and verifying the model performance (WMO 1975, 1986, 1992; Madsen, 2002; Zhang and Guo 2002; Xiong, *et al.* 2002; Xiong and Guo 2004).

Case study

Three watersheds, Luanchuan, Daba, and Shangyi watersheds in semi-humid and semi-arid regions of northern China, were selected to test the model performance. The characteristics for the three watersheds are shown in Table 1. Mean annual precipitation ranges from 375–791 mm, and the runoff coefficients of the Luanchuan, Daba and Shangyi watershed are 0.35, 0.095 and 0.067, respectively.

Luanchuan watershed

The Luanchuan watershed drains an area of 340 km^2 and is characterized by steep slopes (9.78‰). The normal annual rainfall of Luanchuan watershed generally varies between 535–1296 mm. The climatic tendencies produce the highest flooding in the period from July to August. The data for calibration comprised five successive months (Jun.–Oct.) of hourly discharge during 1975–1991 (nine years), while the data of 1992–1993 were used for validation.

Table 1 Characteristics of three watersheds

Watershed	Area (km^2)	P (mm yr^{-1})	Ep (mm yr^{-1})	Runoff (mm yr^{-1})	Runoff coeff.	Climate zone
Luanchuan	340.0	791	1100	276	0.35	Semi-humid
Daba	820.0	522	1087	49	0.095	Semi-humid
Shangyi	16.6	375	1000	25	0.067	Semi-arid

Daba watershed

The Daba watershed, being part of the branch of the Yan River, is located in Anzai county of Shaanxi province. The mean elevation of the watershed is 1400 m. Loss gutter zones with scarce vegetation characterize the main part of the watershed and the soil erosion is significant. Short duration and high intensity rainstorms play an important role in flood events. The Daba hydrological station controls the drainage area (820 km^2). The calibration period considered was three successive months (Jun.–Aug.) of hourly discharges in 2002. There were three successive flood events during this period.

Shangyi watershed

The Shangyi watershed covers 18.5 km^2 and is a branch of the upper Yongding River. It is covered in thick sand and gravel deposits. Generally, rainfall in the monsoon season is about 75–80% of the annual rainfall. The high intensity and short duration storms play an important role in this region, and the surface runoff is always generated by local infiltration excess runoff. The calibration period considered was two successive months (Jul.–Aug.) of discharges with 20 min intervals during 1979–1983. There were twelve main flood events during this period and the data for 1984–1985 were used for validation (including six main flood events).

Simulation results

Table 2 shows the values of R^2 and *RE* for the modified Xinanjiang model. Figures 6 and 7 respectively plot the observed and simulated hydrographs of the Luanchuan watershed in 1975 and the Daba watershed in 2002 during the calibration period, and Figures 8 and 9 plot the observed and simulated hydrographs of the Luanchuan watershed during 1992, and the Shangyi watershed during Aug. 1984 during the validation period.

The modified Xinanjiang model is compared with the original Xinanjiang model, the TOPMODEL and the VIC model (Liang and Xie 2001). The TOPMODEL is rather a set of conceptual tools that can be used to reproduce the hydrological behavior of a watershed in a distributed or semi-distributed way. It is a variable contributing area conceptual model in

Table 2 The simulated results of the modified Xinanjiang model, the original Xinanjiang model, the VIC model and the TOPMODEL

Watershed			Luanchuan	Daba	Shangyi
The original Xinanjiang model	Calibration	R^2 (%)	83.1	92.1	71.9
		RE (%)	0.1	0.0	−0.6
	Validation	R^2 (%)	77.4	–	65.3
		RE (%)	6.3	–	−12.3
The modified Xinanjiang model	Calibration	R^2 (%)	85.3	92.1	78.2
		RE (%)	−0.6	0.0	1.1
	Validation	R^2 (%)	79.3	–	69.4
		RE (%)	4.1	–	−9.2
The VIC model	Calibration	R^2 (%)	82.4	91.1	72.6
		RE (%)	−0.4	0.0	0.0
	Validation	R^2 (%)	71.8	–	67.0
		RE (%)	8.5	–	−14.39
The TOPMODEL	Calibration	R^2 (%)	74.1	78.3	58.97
		RE (%)	4.4	1.6	−0.6
	Validation	R^2 (%)	68.2	–	49.7
		RE (%)	4.5	–	−18.2

(Note: – represents no validation data)

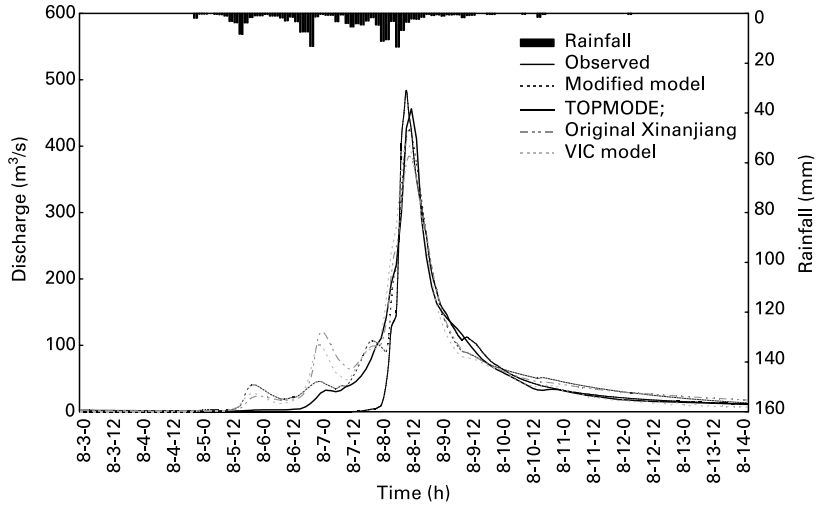

Figure 6 The observed and simulated runoff hydrograph in the Luanchuan watershed (1975, calibration)

which the predominant factors determining the formation of runoff are represented by the topography of the watershed and a negative exponential law linking the transmissivity of the soil with the distance to the saturated zone below the ground level. Sivapalan *et al.* (1990) introduced the use of a gamma distribution in their scaled version of the TOPMODEL. Beven *et al.* (1995) used a gamma distribution in a runoff production function for a flood forecasting model and gave details of a gamma distribution version for continuous simulation. The application of the TOPMODEL in China has been studied and discussed in detail by Xiong *et al.* (2002) and Xiong and Guo (2004). Due to the lack of DEM data in these watersheds, the gamma function was adopted to substitute for the topographical descriptors. The parameters of the TOPMODEL were calibrated by a combination of the Genetic, Rosenbrock and Simplex algorithms, the same as in the calibrated methods of the original Xinanjiang and the modified Xinanjiang models.

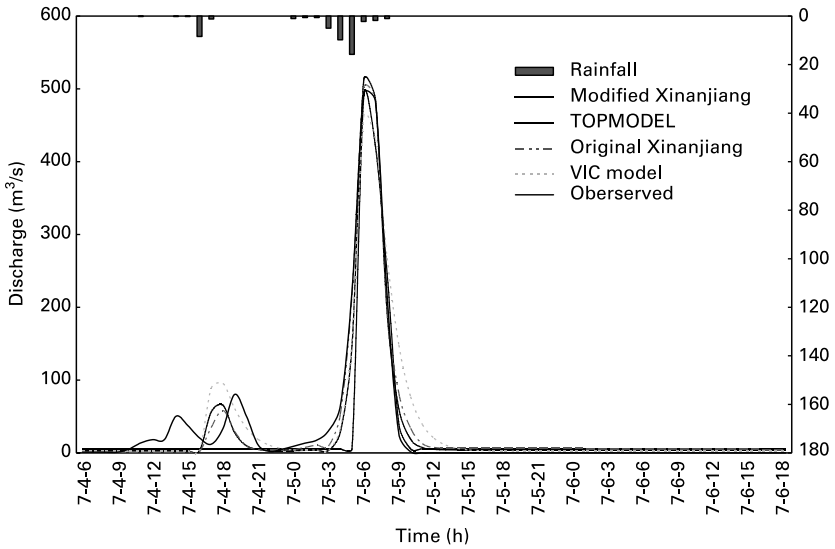

Figure 7 The observed and simulated runoff hydrograph in the Daba watershed (2002, calibration)

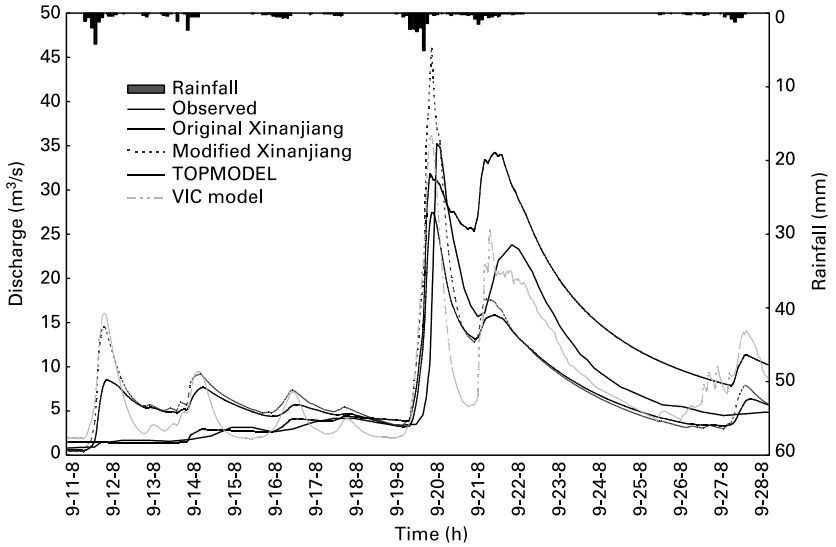

Figure 8 The observed and simulated runoff hydrograph in the Luanchuan watershed(1992, validation)

The VIC model is a land surface runoff parameterization model presented by Liang and Xie (2001, 2003). The model dynamically considers the two major surface runoff generation mechanisms: infiltration excess runoff and saturation excess runoff, within a studied area or a model grid cell. The surface runoff and the sub-surface runoff are routed through the Nash unit hydrograph and linear reservoir. The parameters of the VIC model were calibrated with the same calibrated methods as the other models.

The efficiency R^2 and relative error *RE* of the TOPMODEL and the VIC model for these watersheds were also shown in Table 2 and the simulated flow hydrographs in the calibration and validation periods were plotted in Figures 6–9.

According to Table 2, there is a marginal difference in the results in the Luanchuan (semi-humid) watershed, a small improvement in the Shangyi (semi-arid) watershed and appears to

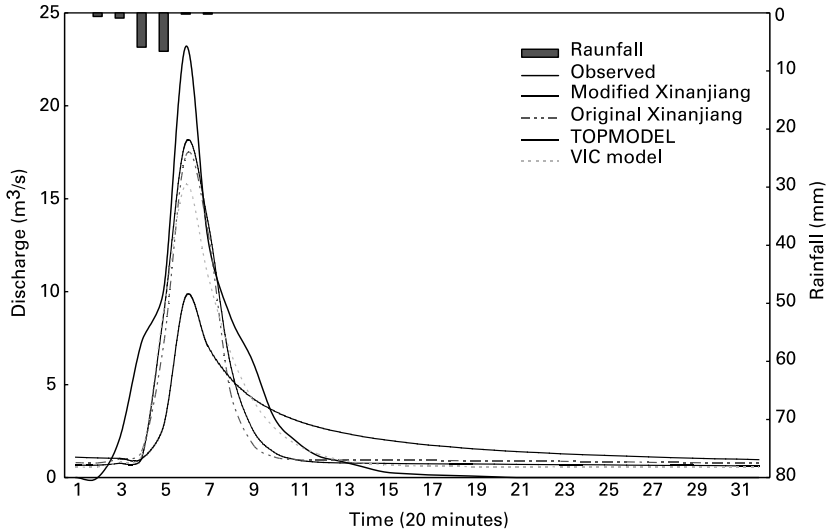

Figure 9 The observed and simulated runoff hydrograph in the Shangyi watershed (22 Aug. 1984, validation)

be a marginal difference in the Daba watershed, in terms of R^2. Also, the improvements in the semi-humid watersheds are smaller than those in the semi-arid watershed. As discussed in the introduction, nearly any proper model can simulate rainfall–runoff relationships of the humid and semi-humid watersheds quite satisfactorily; however, it is not easy to achieve a good simulation result on the semi-arid and arid watersheds because the hydrological processes are much more complex in these regions (Li 1998). The results of this study demonstrated that the modified Xinanjiang model performs better than the original Xinanjiang model in the semi-arid watershed, but not necessarily better than the NAM, HBV and other lumped, conceptual models. Therefore the modified Xinanjiang model may be useful in practice.

Figures 10–13 show the infiltration excess runoff component, saturation excess runoff component and total runoff hydrograph of the modified Xinanjiang model and the VIC model during 8–9 Aug. 1975 in the Luanchuan and Shangyi watersheds. Two types of models have different runoff generation process. From Figures 10–12, it can be seen that the infiltration excess runoff of the modified Xinanjiang model is proportional to rainfall intensity. The initial infiltration rate is generally high at the beginning of the storm when the soil moisture is usually very low. Thus more water can infiltrate into the soil with less water being generated as infiltration excess runoff. Other findings show that the infiltration excess runoff is high when the precipitation intensity is high and the saturation excess runoff is increased with the increase in soil moisture. While the hydrograph of the VIC model shows different simulating results in different climate zones the saturation excess runoff is the main dominant runoff generation method in the Luanchuan watershed (semi-humid), and the infiltration excess runoff is the main runoff generation area in the Shangyi watershed (semi-arid).

Discussions and conclusions

The modified Xinanjiang model, which considers two major mechanisms of runoff generation simultaneously in the semi-humid and semi-arid regions, is presented in this paper. Some discussions and conclusions of this study are summarized as follows.

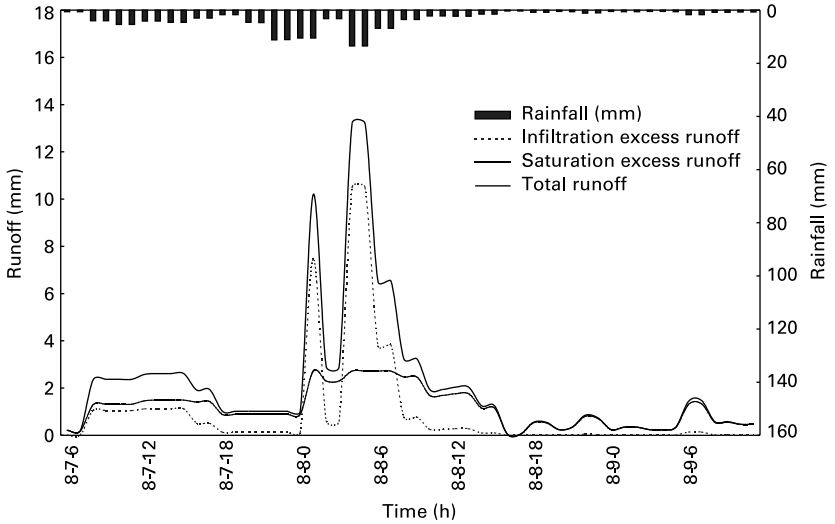

Figure 10 The hydrograph of the infiltration excess runoff component, saturation excess runoff component and total runoff of the modified Xinanjiang model (1975, Luanchuan)

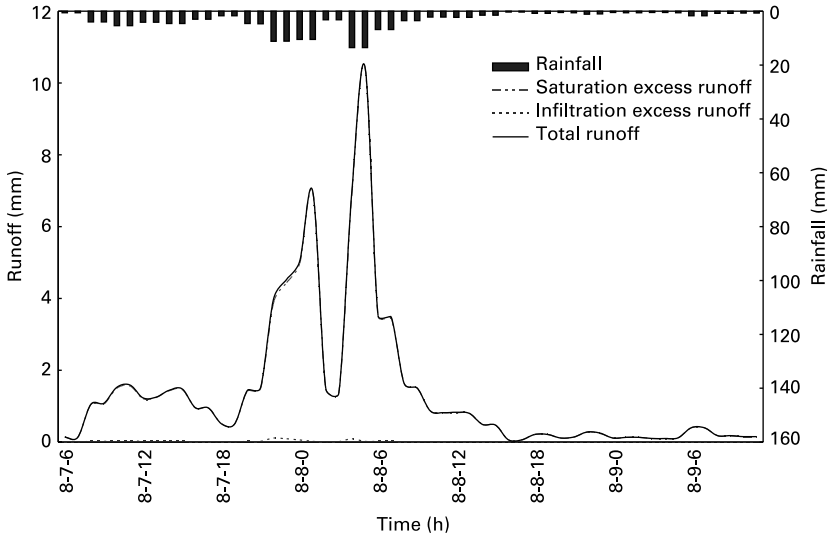

Figure 11 The hydrograph of the infiltration excess runoff component, saturation excess runoff component and total runoff of the VIC model (1975, Luanchuan)

The modified Xinanjiang model is different from the ARNO model (Todini 1996) and the VIC model (Liang and Xie 2001, 2003). The ARNO model just takes the saturation excess runoff into account on surface runoff in a watershed and considers the drainage and percolation losses in the soil moisture balance. The VIC model considers the saturation excess runoff and the infiltration excess runoff at different locations of a studied area due to the spatial variability of the soil infiltration rate and soil moisture capacity, and the total surface runoff is the sum of the saturation excess runoff and the infiltration excess runoff. While the modified Xinanjiang model considers both Horton and Dunne runoff generation mechanisms simultaneously, and assumes that the Horton runoff occurs if the rainfall intensity rate is greater than the infiltration rate, the Dunne runoff is generated if the soil

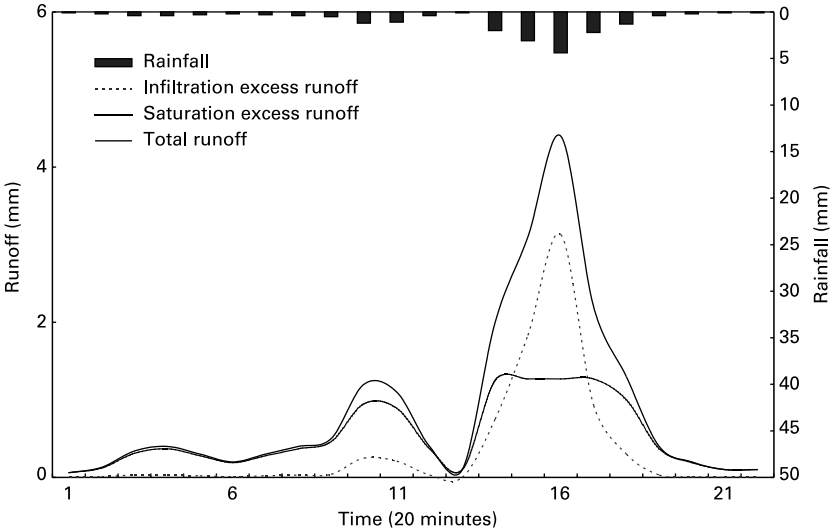

Figure 12 The hydrograph of the infiltration excess runoff component, saturation excess runoff component and total runoff of the Xinanjiang model (24 Jun. 1982, Shangyi)

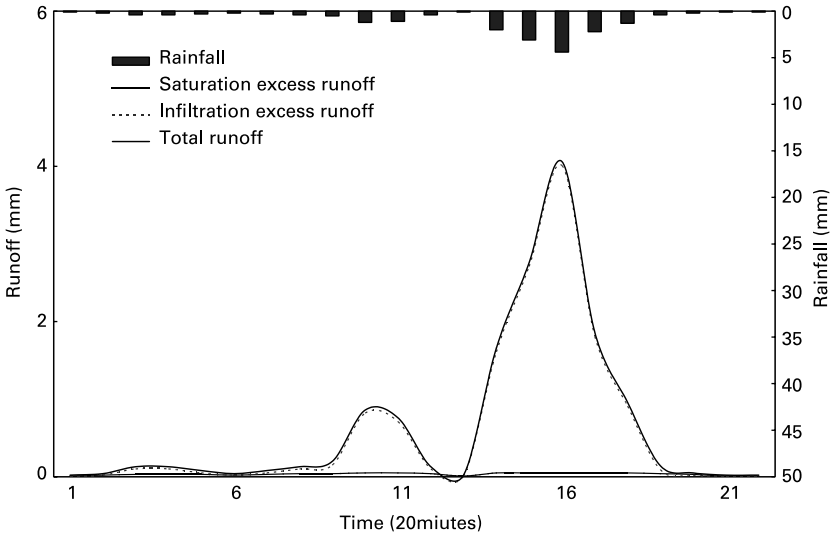

Figure 13 The hydrograph of the infiltration excess runoff component, saturation excess runoff component and total runoff of the VIC model (24 Jun. 1982, Shangyi)

moisture content of the aeration zone reaches field capacity in the watershed. Two types of models reflect different runoff generation mechanisms.

The VIC model and the TOPMODEL were also calibrated for the three test watersheds and their results were compared with those of the original Xinanjiang model and the modified Xinanjiang model. It is found that the results of the TOPMODEL are poorer than those of the original Xinanjiang model, the modified Xinanjiang model and the VIC model, especially in the Shangyi watershed. The reason for the poor performance of the TOPMODEL may be due to the lack of DEM data. It is also found that the results of the models considering the Horton and Dunne runoff generation mechanisms are slightly better than those of the original Xinanjiang model considering the single runoff generation mechanism in semi-arid regions.

In conclusion, the modified Xinanjiang model, whose runoff generation mechanism is based on both infiltration excess and saturation excess runoff, is a flexible tool for rainfall–runoff simulation in semi-arid and semi-humid regions in northern China, especially for semi-arid watersheds.

Acknowledgements

The study is supported by the Chinese National Key Basic Research Fund (G19990436), the Chinese Natural Research Fund (50179026) and the Open Research Fund Program of State Key Laboratory of Water Resources and Hydropower Engineering Science of China (2003C002). The authors are very grateful to the editor and two anonymous referees whose comments and improvement of the text helped to clarify and improve the paper.

References

Abdul, A.S. and Gillham, R.W. (1984). Laboratory studies on the effects of the capillary fringe on streamflow generation. *Wat. Res. Res.*, **20**(6), 691–698.

Atkinson, S.E., Woods, R.A. and Sivapalan, M. (2002). Climate and landscape controls on water balance model complexity over time scales. *Wat. Res. Res.*, **38**(12), 101029/2002WR001487.

Beldring, S. (2002). Runoff generating processes in Boreal forest environment with glacial tills. *Nord. Hydrol.*, **33**(5), 347–372.

Beldring, S., Gottschalk, L., Seibert, J. and Tallaksen, L.M. (1999). Distribution of soil moisture and groundwater levels at patch and catchment scales. *J. Agric. Forest Meteorol*, **98–99**, 305–324.

Bergström, S. (1991). Principles and confidence in hydrological modeling. *Nord. Hydrol.*, **22**(2), 123–136.

Bergström, S. and Forsman, A. (1973). Development of a conceptual deterministic rainfall-runoff model. *Nord. Hydrol.*, **4**, 147–170.

Beven, K.J. (1989). Changing ideas in hydrology—the case of physically-based models. *J. Hydrol.*, **105**, 157–172.

Beven, K.J. and Kirkby, M.J. (1979). A physically-based variable contributing area model of basin hydrology. *Hydrol. Sci. Bull.*, **24**(1), 43–69.

Beven, K.J., Lamb, R., Quinn, R., Romanowicz, R. and Freer, J. (1995). TOPMODEL. In *Computer Models of Watershed Hydrology*, V.P. Singh (ed.), Water Resources Publication, Highlands Ranch, CO, pp. 627–668.

Burnash, R.J.C., Ferral, R.L. and Guire, R.A. (1973). A general streamflow simulation system-conceptual modeling for digital computers. *Report* Joint Federal State River Forecasts Center, Sacramento.

Crawford, N.H. and Linsly, R.S. (1966). Digital simulation in hydrology: the Stanford watershed model. *Technical report no.* 39. Department of Civil Engineering, Stanford University, Palo Alto, CA.

Dunne, T. (1978). Field studies of hillslope flow processes. In *Hillslope Hydrology*, M.J. Kirkby (ed.), Wiley, New York, pp. 227–293.

Farmer, D., Sivapalan, M. and Jothityangkoon, C. (2003). Climate, soil and vegetation controls upon the variability of water banlance in temperate and semi-arid landscapes: downward approach to hydrological prediction. *Wat. Res. Res.*, **39**(2), 101029/2001WR000328.

Feldman, A.D. (1981). HEC Models for Water Resources System Simulation:Theory and Experience. In *Advances in Hydroscience*, Ven Te Chow (ed.), (**12**), Academic Press, New York, pp. 297–423.

Franchini, M. and Pacciani, M. (1991). Comparative analysis of several conceptual rainfall-runoff models. *J. Hydrol.*, **122**, 161–219.

Freeze, R.A. (1980). A stochastic-conceptual analyse of rainfall-runoff processes on a hillslope. *Wat. Res. Res.*, **16**(2), 391–408.

Hu, F., Xia, P. and Shen, Y. (1986). Discussing on Xinanjiang model of four water resources and geography laws of the parameter. *Chinese J. Hydrol.*, **1**, 16–24.

M.J. Kirkby (ed.), (1978). Hillslope Hydrology, Wiley, New York.

Li, Q. (1998). Analysis and discussion related to the hydrological watershed models used in the first Hydrological Forecasting Technology Competition of China. *Chinese Adv. Wat. Sci.*, **9**(2), 187–195.

Liang, X. and Lettenmaier, D.P. (1994). A simple hydrologically based model of land surface water and energy fluxes for general circulation models. *J. Geophy. Res.*, **99**(D7), 14415–14428.

Liang, X., Lettenmaier, D.P. and Wood, E.F. (1996). Surface soil moisture parameterization of the VIC-2L model: evaluation and modifications. *Global Planet. Change*, **13**, 195–206.

Liang, X. and Xie, Z. (2001). A new surface runoff parameterization with subgrid-scale soil heterogeneity for land surface models. *Adv. Wat. Res.*, **24**, 1173–1193.

Liang, X. and Xie, Z. (2003). Important factors in land-atmosphere interactions: surface runoff generations and interactions between surface and groundwater. *Global and Planetary Change*, **38**(1–2), 101–114.

Luo, W., Hu, C. and Han, J. (1992). Research on a model of runoff yield reflecting excess infiltration and excess storage simultaneously. *Chinese J. Soil Wat. Conserv.*, **6**(4), 6–13.

Madsen, H. (2002). Automatic calibration of a conceptual rainfall-runoff model using multiple objectives. *J. Hydrol.*, **235**, 276–288.

Nash, J.E. and Sutcliffe, J.V. (1970). River flow forecasting through conceptual models. *J. Hydrol.*, **10**, 282–290.

Nielsen, S.A. and Hansen, E. (1973). Numerical simulation of rainfall runoff process on a daily basis. *Nord. Hydrol.*, **4**, 171–190.

Refsgaard, J.C. (1996). Terminology, modeling protocol and classification of hydrological model codes. In *Distributed Hydrological Modeling*, M.B. Abbott and J.C. Refsgaard (eds.), Kluwer, Dordrecht, pp. 17–39.

Rockwood, D.M. (1982). Theory and practice of the SSARR model as related to analyzing and forecasting the response of hydrologic systems. *Proceedings of the International Symposium on Rainfall-runoff Modeling*, May 1981. Mississippi State University.

Rui, X. and Jiang, G. (1997). Some development of the theories and computation methods in runoff yield. *Chinese J. Hydrol.*, **4**, 16–20.

Singh, V.P. (1995). *Computer Models of Watershed Hydrology*, Water Resources Publications, Highlands Ranch, CO.

Singh, V.P. and Frevert, D.K. (2002). *Mathematical Models of Large Watershed Hydrology*, Water Resources Publications, Denver, CO.

Sittner, W.T., Schauss, C.E. and Monro, J.C. (1969). Continues hydrograph synthesis with an API-type hydrological model. *Wat. Res. Res.*, **5**(5), 1007–1022.

Sivapalan, M., Beven, K. and Wood, E.F. (1987). On hydrologic similarity 2. a scaled model of storm runoff production. *Wat. Res. Res.*, **23**(12), 2266–2278.

Sivapalan, M., Wood, E.F. and Beven, K. (1990). On hydraulic similarity 3. A dimensionless flood frequency model using a generalized GUH and partial area runoff generation. *Wat. Res. Res*. **26**(1), 43–58.

Sugawara, M. (1974). Tank model and its application to Bird Creek, Wollombi Brook, Bikin River, Kitsu River, Sanaga River, Sanaga River and Nam Mune. Research note of the National Research Center for diaster prevention, No. 11. pp. 1–64

Todini, E. (1988). Rainfall runoff modeling: past, present and future. *J. Hydrol.*, **100**, 341–352.

Todini, E. (1996). The ARNO rainfall-runoff model. *J. Hydrol.*, **175**, 339–382.

Wang, P. (1982). Applied test on Xinanjaing model of the three water resources. *Chinese J. Hydrol.*, **5**, 24–31.

Wang, P. and Zhao, R. (1989). Impersonality optimizing method on the parameter of Xinanjiang model (three water resources). *Chinese J. Hehai Univ.*, **17**(4), 65–69.

World Meteorological Organization. (WMO 1975). Intercomparison of conceptual models used in operational hydrological forecasting. *WMO Oper. Hydrol. Rep.* 7, WMO 429

World Meteorological Organization. (WMO 1986). Intercomparation of models for snowmelt runoff. *WMO Oper. Hydrol. Rep.* 23, WMO 646.

World Meteorological Organization. (WMO 1992). Simulated real-time intercomparison of hydrological models. *WMO Oper. Hydrol. Rep.* 38, WMO 779.

Xiong, L. and Guo, S. (2004). Effects of the catchment runoff coefficient on the performance of TOPMODEL in rainfall-runoff modeling. *Hydrol. Process.*, **18**, 1823–1836.

Xiong, L., Guo, S. and Hu, C. (2002). Application and studies of TOPMODEL in runoff simulation on different watersheds. *Chinese J. Hydrol.*, **22**(5), 5–8.

Zhang, H. and Guo, S. (2002). Automatic calibration methods for multiple objectives of conceptual hydrological model. *Chinese J. Hydrol.*, **22**(1), 12–16.

Zhao, R. (1980). The Xinanjiang model. *Proceedings Oxford Symposium. IAHS Publ.*, **129**, 351–356.

Zhao, R. (1992). The Xinanjiang model applied in China. *J. Hydrol.*, **135**, 371–381.